# An Active Parallel Power Decoupling Circuit for Single Stage AC-PV Modules

Nasser Ghasemi, Mahdi Akhbari
Electrical and Electronic Engineering Department
Shahed University
Tehran, Iran
Naserghasemi2012@gmail.com

***Abstract*—AC photovoltaic modules due to several advantages in compare to centralized PV systems and string PV systems are future trend. Microinverters are important component of an AC-PV module. Output power at single phase single stage grid connected microinverters is pulsating with twice grid voltage frequency whereas the PV module produced power is constant. In conventional design a power decoupling capacitor handle difference input and output power, this causes the PV current and the power decoupling capacitor voltage be fluctuating. This problem influences the operation of maximum power tracking of PV module and increases output current THD. However a bulky PV side power decoupling capacitor can reduce voltage ripple; but using a big electrolytic capacitor reduces converter lifetime and system reliability and as well as increases microinverter volume and cost. In this paper a novel parallel power decoupling circuit based on flyback topology is proposed to reduce the decoupling capacitor size and voltage ripple. This circuit operates as a controlled current source in parallel with PV module. Proposed circuit controller is independent from main microinverter and utilizes a simple control strategy without any additional sensor. By employing proposed circuit on flyback microinverter, low frequency voltage fluctuating is mitigated without usage of a big capacitor. For verifying proper operation of the proposed circuit, the whole of the flyback microinverter with active decoupling circuit as well as their control circuits are modeled in PowerSim software, the circuit operation is simulated. Proper functioning of the circuit and the expected performances issued from simulation results proved in all conditions.**

***Keywords—active power docoupling circuit; low frequency voltage ripple; decopling capacitor; AC-PV module; single stage microinverter; maximum power point tracking( MPPT)***

## I. INTRODUCTION

Nowadays renewable energy systems including photovoltaic systems are getting very popular because of global energy shortage trend and energy demand rising. They have vital advantages such as being sustainable, pure and suitable for small-scale applications [1]. PV energy systems are classified to centralized systems, string systems and AC-PV modules [1]. AC-PV modules can be used in residential applications, distributed generations and even centralized big PV power plants. AC modules are based on microinverters and have important advantages such as no need to DC power distribution line, elimination of PV modules mismatch affect, overcoming string modules shading effect, decreasing installation cost and improving system efficiency[2],[3].

AC-PV Modules usually use a microinverter to connect utility grid. The microinverter have to be simple and high efficient and furthermore have a long lifetime. Thus lots of topologies are proposed for microinverters [4]-[6]. These topologies in terms of power processing units categorize to single stage microinverters and two or more stage microinverters. Single stage microinverters are very attractive for researchers because they have minimum components and low energy losses.

Output power at single phase single stage microinverters is variable with low frequency (twice grid frequency) while the PV module instantaneously power is constant. Therefore a big capacitor is required to handle difference instantaneous power pulsation. Using big electrolytic capacitor decreases system reliability and lifetime. Moreover decoupling capacitor voltage pulsating can cause two problems: increasing the output current distortion and decreasing PV module power utilization in turns can reduce the output power quality and MPPT efficiency respectively [7].

For solving mentioned problem many circuits are proposed to reduce power decoupling capacitor size and then use small film capacitors substitute of limited lifetime electrolytic capacitors [3], [8], [9]. According to decoupling capacitor location, active power decoupling circuits classify to three main groups: 1) DC-Link decoupling circuits; 2) PV Side decoupling circuits and 3) AC Side decoupling circuit. DC-Link decoupling circuits add one extra power processing stage to microinverter topology and AC Side decoupling circuits need sophisticated control schemes. But PV Side power

decoupling methods are best way from efficiency aspect and have low control complexity in compare to another two methods [8]. Some PV side decoupling circuits have been presented in the literature [3], [9]-[12]. In some references the switching frequency of decoupling circuit is considered to be equal to main microinverter circuit switching frequency, therefore power loss is significant. In addition most of them are especially designed to their proposed microinverter, thus they are not appropriate for other microinverters [3], [10] and [11]. Also some of the proposed circuits for power decoupling have complex control strategy or lots of active components. Fig. 1(a) and (b) demonstrate two types of mentioned circuits that are called Buck-Boost and Full-Bridge RCR(ripple current reduction) respectively [12].

In this paper a PV module paralleled flyback based active power decoupling circuit is proposed for reducing the decoupling capacitor size and improving reliability and lifetime of AC-PV modules. This circuit can be used generally for all single stage AC module microinverters and have low components in compare to similar decoupling circuits. In addition at each time, one of the decoupling circuit switches operates at low frequency, therefore power loss is minimized by this circuit. Control strategy of the proposed decoupling circuit does not need any extra sensor and is operating independent of main microinverter circuit. This circuit is presented and tested on single stage flyback microinverter by simulation using PowerSim software. Simulations results illustrate that the proposed decoupling circuit effectively reduces the PV Module voltage ripple and with this circuit small film capacitor may be used as DC decoupling capacitor.

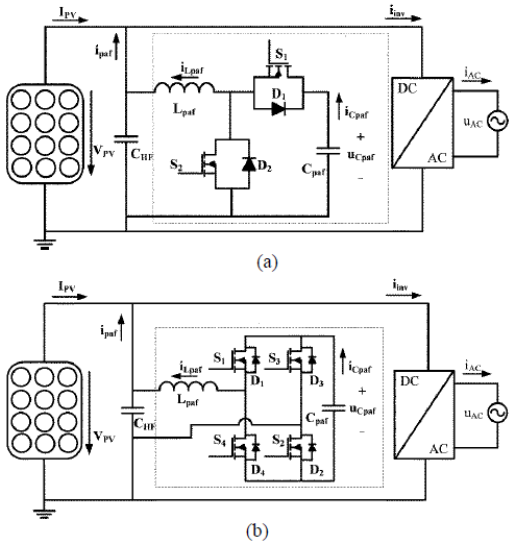


Fig. 1. Two types of active power decoupling circuits (a) Buck-Boost RCR, (b) Full-Bridge RCR

## II. PROPOSED DECOUPLING CIRCUIT PRINCIPLES

### A. *Power Decoupling circuit*

Fig. 2 Shows grid connected photovoltaic microinverter with proposed power decoupling circuit. Microinverter has connected PV module to utility by a DC/AC single stage microinverter and an inductor as harmonic filter. Hashed line demonstrates the proposed active decoupling circuit at PV side which handles the low frequency variable power to reduce the decoupling capacitor size and remove the PV voltage ripple. The microinverter can be an optional topology that it is enough to be single-phase and single stage. $C_{PV}$ is power decoupling capacitor that must have a high capacity if an additional power decoupling circuit is not considered in microinverter. Proposed decoupling circuit is based on flyback topology that is similar to a bidirectional converter, it operates so that to be a controlled current source (see Fig. 3). This circuit consists of two switches, $S_{d1}$ *and* $S_{d2}$, an inverted transformer and capacitor $C_d$. At positive polarity of power decoupling reference current ($I_d(t)$) only $S_{d2}$ is switching at high frequency and the other switch is off. In this mode the converter operates as a buck converter and discharge the energy stored in $C_d$ capacitor to the microinverter. In contrary when the power decoupling reference current ($I_d(t)$) polarity is negative only the $S_{d1}$ is switching at high frequency and in this mode the power decoupling circuit is operating as a boost type converter. In this mode energy flows from PV module to the $C_d$ capacitor. In both modes flyback converter operates at discontinuous conduction mode (DCM) and therefore the antiparallel diodes of the switches do not have reverse recovery losses. In both modes decoupling circuit can operate at a frequency several times lower the microinverter switching frequency.

### B. *Decoupling capacitor sizing In the absence of power decoupling circuit*

By considering the utility grid voltage and output current a pure sine wave with RMS values of $V_g$ and $I_g$ respectively and $\varphi$ as their phase difference:

$$v_g = \sqrt{2} V_g \sin \omega t \qquad (1)$$

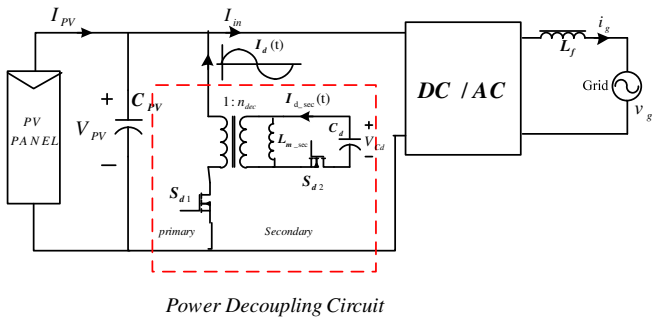


Fig. 2. Microinverter with proposed power decoupling circuit

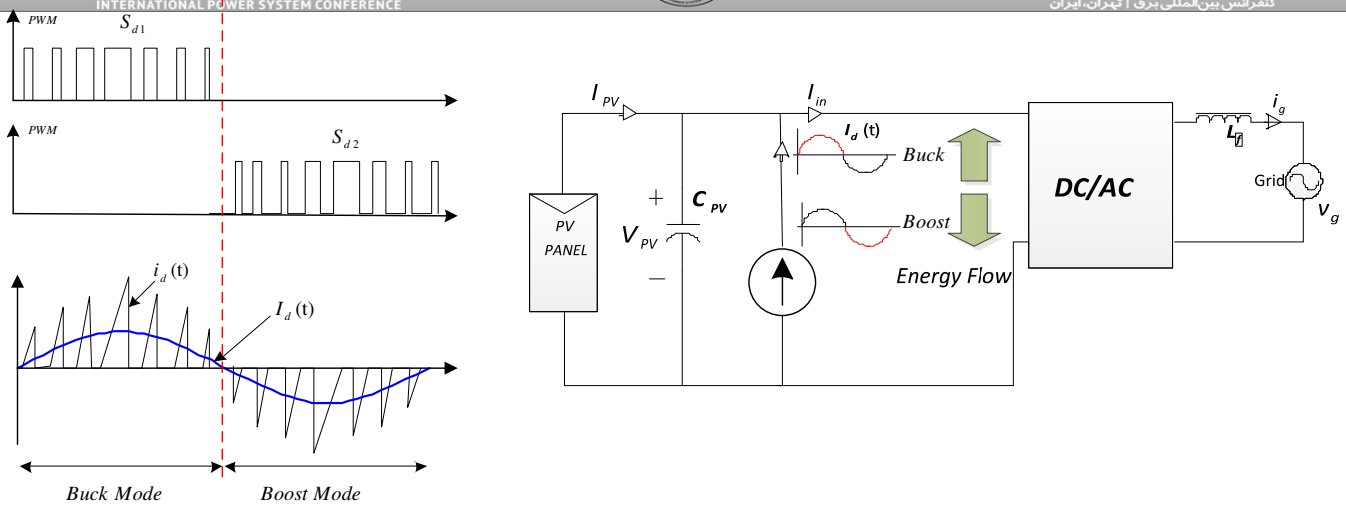


Fig. 3. Proposed power decoupling switching, current waveforms and energy flow in buck and boost mode

Instantaneous output power can be obtained by:

$$p_o(t) = V_g I_g (\mathrm{Cos}\,\varphi - Cos(2\omega t + \varphi)) \quad (3)$$

In microinverters usually the output power factor is unit, so output current phase ( $\varphi$ ) can be neglected. Thus the output power equation can be simplified to:

$$p_o(t) = V_g I_g - V_g I_g Cos(2\omega t) = P_{avg} - P_{avg} Cos(2\omega t) \quad (4)$$

$$p_{in}(t) = p_o(t) \quad (5)$$

According to equation (4) the output power consists of two terms. Assume that efficiency is 100%, the input power will be equal to the same expression. First term is the average power which is equal to PV power at maximum power point and the second term is a pulsation power with twice grid voltage frequency. Pulsation power has to be handled by decoupling capacitor in lack of any power decoupling circuit. According to Fig. 4, the energy difference of PV power and instantaneous power at each period is equal to energy difference of $C_{PV}$ capacitor between minimum and maximum voltage. Therefore:

$$\frac{1}{2}C_{PV}V_{PV\max}^2 - \frac{1}{2}C_{PV}V_{PV\min}^2 = \frac{1}{\pi}\int_{\pi/4}^{3\pi/4}(P_{avg} - P_{avg}\,Cos\,2\omega t)\,d(\omega t) \quad (6)$$

Where in $V_{PV}$ is PV module voltage. By multiplying equation (6) to twice frequency of grid voltage, average power equation will be:

$$f_g C_{PV} V_{PV\max}^2 - f_g C_{PV} V_{PV\min}^2 = \frac{1}{\pi} P_{avg} \quad (8)$$

Where in $f_g$ is grid voltage frequency and $V_{PVmax}$ and $V_{PVmin}$ are defined by:

$$V_{PV\max} = V_{PV} + \frac{\Delta V_{PV}}{2} \quad (9)$$

$$V_{PV\min} = V_{PV} - \frac{\Delta V_{PV}}{2} \quad (10)$$

Then voltage ripple of power decoupling capacitor ( $\Delta V_{PV}$ ) can be calculated by:

$$\Delta V_{PV} = \frac{P_{avg}}{2\pi f_g V_{PV} C_{PV}} \quad (12)$$

Therefore a complete expression for capacitor voltage (PV voltage) is:

$$v_{PV}(t) = V_{PV} - \frac{\Delta V_{PV}}{2} Sin(2\omega t) \quad (13)$$

Equation (13) illustrates obviously the PV voltage has a variable term fluctuating with twice grid frequency. The amplitude of this term ( $\frac{\Delta V_{PV}}{2}$ ) is significant against the DC-link type capacitors, this is due to the average voltage of

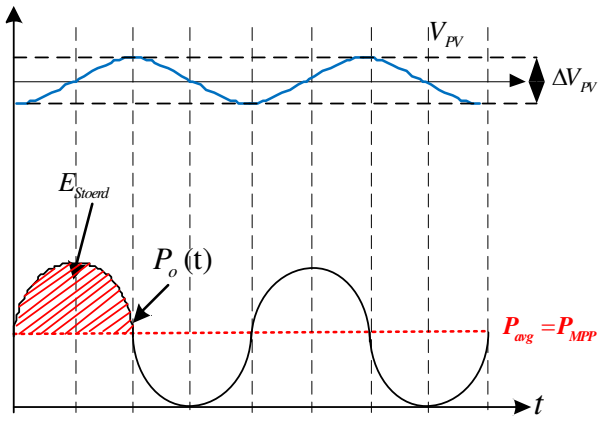


Fig. 4. Output power and PV voltage ripple waveforms

capacitor ($V_{PV}$) is low in single stage microinverters. Proposed decupling circuit in this paper increases the average voltage of decoupling capacitor, therefore capacitor voltage ripple and capacitor size is reduced.

### C. power decoupling reference current

Now by considering the input required power as equation (14):

$$P_{in}(t) = v_{PV}(t) I_{in}(t) = V_{PV} I_{in}(t) - \frac{\Delta V_{PV}}{2} I_{in}(t) \operatorname{Sin} 2\omega t \quad (14)$$

Where in $I_{in}(t)$ is the input current of microinverter depicted in Fig. 2 and $v_{PV}(t)$ is substituted by (13). By assuming that the decoupling capacitor eliminates PV voltage ripple completely ($\Delta V_{PV} = 0$) and considering the input current has two terms same as in (15), and use input power expression from (4), the AC term of input current can be derived as:

$$I_{in}(t) = I_{in\_avg} + I_{in\_ac}(t) \quad (15)$$

$$I_{in\_ac}(t) = -\frac{P_{avg}}{V_{PV}} Cos(2\omega t) \quad (16)$$

For fixing the PV voltage, the reference current that must be injected to microinverter is equal to $I_{in\_ac}(t)$, i.e:

$$I_d(t) = I_{in\_ac}(t) \quad (17)$$

According to (17) when the polarity of $I_d(t)$ is positive, the converter have to operate in buck mode and inject the required current to the microinverter, and when the $I_d(t)$ polarity is negative the converter have to operate in boost mode and absorb the current from the microinverter (see Fig. 3). The next sections calculate the reference current and duty cycles in buck and boost mode respectively.

### D. Calculation of buck and boost mode duty cycle

In half AC cycle where buck mode is active, the secondary side average reference current (depicted at Fig. 3) will be:

$$I_{d\_sec}(t) = \frac{P_{avg}}{V_C} \left| Cos\, 2\omega t \right| \quad (18)$$

On the other hand at DCM operation of flyback converter as illustrated in Fig. 5, the secondary side average current can be derived as:

$$I_{sec}(t) = \frac{1}{2} \frac{V_{Cd}}{L_{m\_sec} f_{sd}} D^2_{buck}(t) \quad (19)$$

Where in $f_{sd}$ is switching frequency, $L_{m\_sec}$ is transformer magnetizing inductance at secondary side and $D_{buck}(t)$ is buck mode duty cycle. Then from (19) buck mode duty cycle will be as follows:

$$D_{buck}(t) = \frac{1}{V_C} \sqrt{2 L_{m\_sec} f_{sd} Cos\, 2\omega t} \quad (20)$$

With same analysis when the boost mode is active the primary side reference current in each half cycle will be:

$$I_{d\_pri}(t) = \frac{P_{avg}}{V_{PV}} \left| Cos\, 2\omega t \right| \quad (21)$$

Meanwhile according to Fig. 5 this current can be explained by (22), where in $L_{m\_pri}$ and $D_{boost}(t)$ are magnetizing inductance at primary side and boost mode duty cycle respectively.

$$I_{pri}(t) = \frac{1}{2} \frac{V_{PV}}{L_{m\_pri} f_{sd}} D^2_{boost}(t) \quad (22)$$

Then by substituting (21) into (22) the boost mode duty cycle is will be:

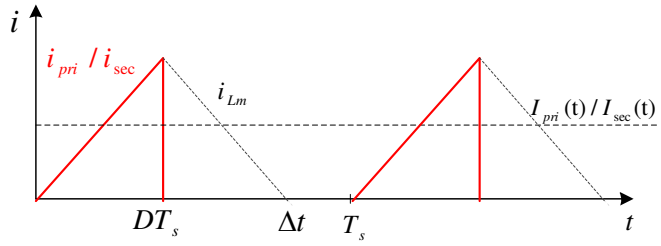


Fig. 5. Power decoupling circuit primary current waveform and magnetizing inductance current waveform

$$D_{boost}(t) = \frac{1}{V_{PV}} \sqrt{2 L_{m\_pri} f_{sd} Cos\, 2\omega t} \quad (23)$$

### E. Power decoupling capacitor sizing

Secondary side current of power decoupling circuit can be obtained as follows:

$$I_{d\_sec}(t) = -\frac{P_{avg}}{n V_{PV}} Cos(2\omega t) \quad (24)$$

Where in "$n$" is transformer turn ratio i.e. $n_1 / n_2$. $I_{d\_sec}(t)$ is flowing from $C_d$ capacitor, thus equation (24) is equal to capacitor current:

$$C_d \frac{dv_{Cd}}{dt} = I_{d\_sec}(t) \quad (25)$$

By solving (25) for capacitor voltage the relation (26) is obtained. This voltage contains a constant term that is $V_{Cd}=nV_{PV}$, and an oscillating term with twice line frequency.

$$v_{Cd}(t) = -\frac{P_{avg}}{2\omega n V_{PV} C_d} Sin\, 2\omega t + V_{Cd} \quad (26)$$

By considering $\Delta V_{Cd}$ as peak to peak voltage oscillation of power decoupling capacitor, and using (26), $C_d$ can be derived by:

$$C_d = \frac{P_{avg}}{\omega n V_{PV} \Delta V_{Cd}} \quad (27)$$

Equation (27) shows that the size of $C_d$ (power decoupling circuit capacitor) is very smaller than $C_{PV}$ (without the presence power decoupling circuit) because the $C_d$ average voltage is higher than $C_{PV}$ average voltage.

## III. CONTROLL STRATEGY

Fig. 6 shows the control strategy of the proposed power decoupling circuit. According to this strategy, at first operating mode determines by calculation of AC grid injected power. Then depending the interval of buck or boost mode, related reference currents are calculated and then duty cycles are derived and applied into the power decoupling circuit

switches by using sine wave pulse width modulation (SPWM). Fig. 7 shows the block diagram of controller structures for both microinverter and proposed circuit. Controllers assigned to the proposed power decoupling circuit and the microinverter circuit are independent. Moreover proposed circuit controller does not require extra feedback and sensor. The detail of control strategy of the microinverter is explained [7].

## IV. SIMULATION RESULTS

To verify the validity of the proposed active power decoupling circuit, it is employed and tested in a single stage flyback microinverter by simulation. The proposed circuit with flyback microinverter are as shown in Fig. 7. This microinverter is classified into single stage microinverters, and need a power decoupling component at PV or AC side [7].

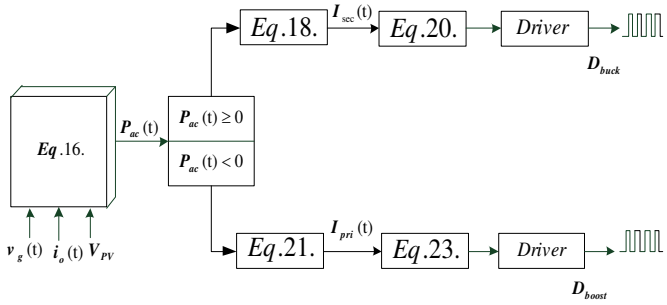


Fig. 6. Control structure for proposed active power decoupling circuit

Microinverter and power decoupling circuit components aresized for 150W rated power connected to 220V/50Hz utility grid. The results of component sizing are presented in Table. 1.

At first microinverter is simulated without using the proposed power decoupling circuit. According to voltage ripple calculation discussed in section II.B, power decoupling capacitor is calculated to be 4.4mF, for peak to peak voltage ripple of 12 percent. In this case with no decoupling circuit some poor results regarding the injected current to the grid are obtained from simulations (output current THD is about 8.5%). Waveforms of Fig. 8(a) shows the output current injected to utility grid with its reference, and Fig. 9(a) shows the PV voltage ripple when power decoupling circuit is not used.

The microinverter by employing proposed active power decoupling circuit with specifications listed in Table. 1 is considered and its performance in the same operating point i.e. 150W output power is simulated. The output current and PV voltage ripple waveforms are illustrated in Fig. 8(b) and Fig. 9(b) respectively. This figures show despite to reducing power decoupling capacitor from 4.4mF to 100uF, the output current waveform quality is significantly improved and the voltage ripple is reduced from about 6V to 1V. These improvements shows a reduction of output current THD from 8.53% to 2.19% and accordingly an enhancement of the MPPT efficiency to harvest maximum energy from PV module estimated about 8%.

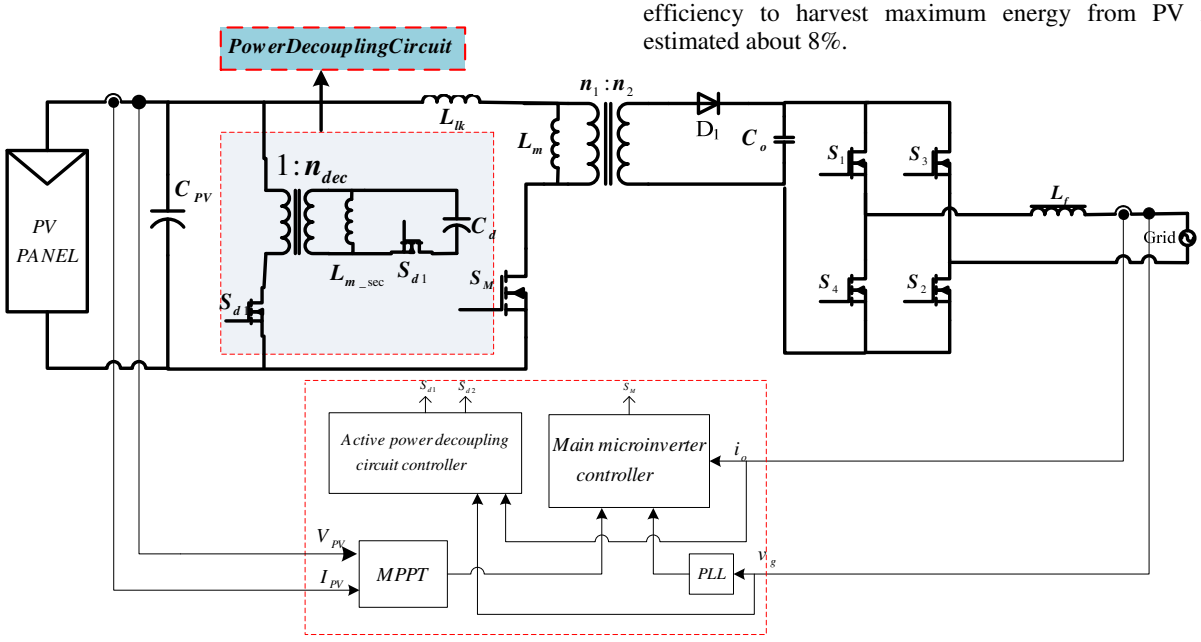


Fig. 7. Flyback micoinverter and proposed active power decoupling circuit controllers overview

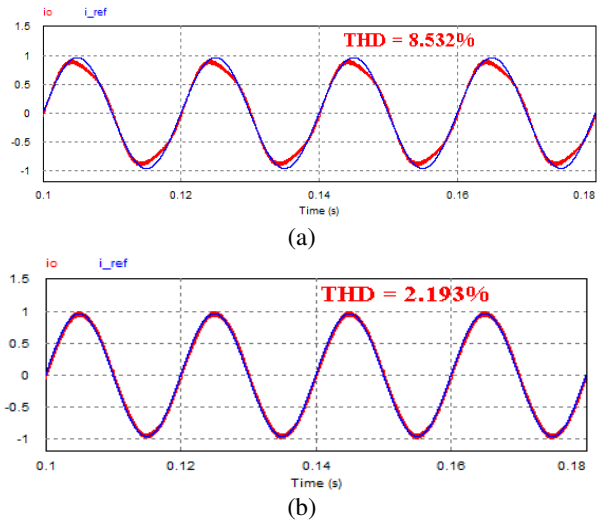


Fig. 8. Output current and its reference: (a) Without active power decoupling circuit. (b) With active power decoupling circuit

Fig. 10 demonstrate power decoupling circuit current and its average reference and Fig. 11 shows the power decoupling circuit capacitor ($C_d$) voltage. These waveforms exhibit properly operating of microinverter and proposed circuit as expected.

For testing microinverter operating in transient and steady state, its behaviors is analyzed in an output power change by applying a step change. Fig. 12 shows transient response of a 50% to 100% rated power step applied to the microinverter load in the presence of proposed decoupling circuit at 0.3s instant. As the results demonstrate, the system recovers the steady state rapidly in a half cycle (about 10ms) without any overshoot. Moreover this figure shows that proposed circuit operates appropriately at both power levels.

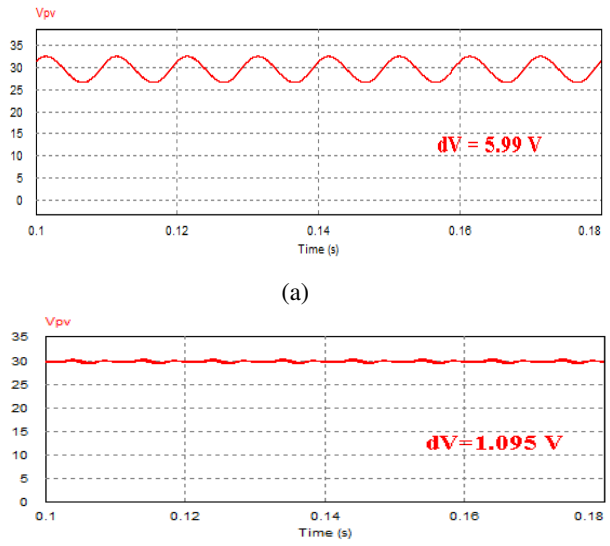


Fig. 9. (b) PV voltage ripple: (a) Without active power decoupling circuit. (b) With active power decoupling circuit

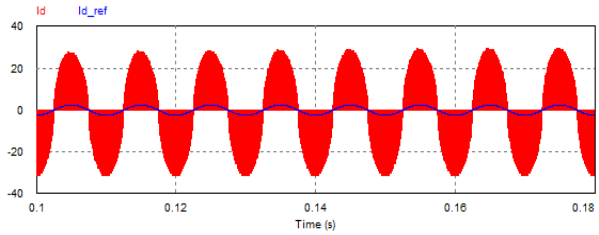


Fig. 10. Active power decoupling circuit current and its reference current

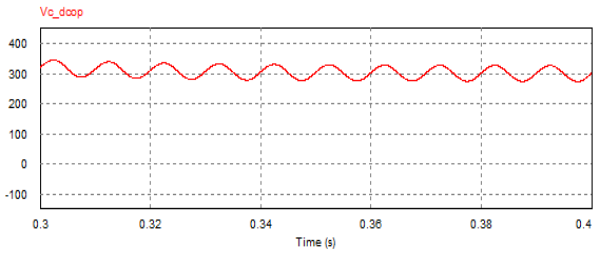


Fig. 11. Active power decoupling circuit capacitor ($C_d$) voltage waveform

TABLE I. MICROINVERTER AND ACTIVE POWER DECOUPLING CIRCUIT PARAMETERS

| *Parameter* | Value |
|---|---|
| $P_{rated}$ | 150W |
| $V_{PV}$ | 30V |
| $V_{grms}$ | 220V |
| $f_g$ | 50Hz |
| $C_d$ | 30uF |
| $f_d$ | 30KHz |
| $n$ | 4 |
| $f_s$ | 75KHz |
| $C_f$ | 680nF |
| $L_f$ | 600uH |
| $C_{PV}$ | 100uF |

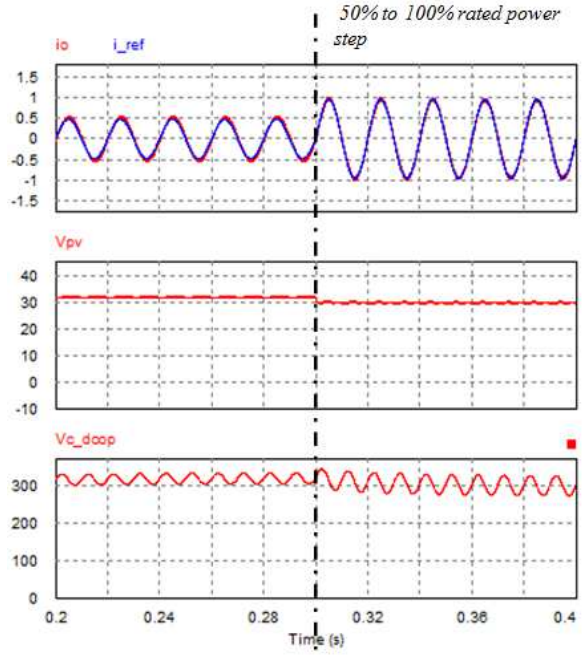


Fig. 12. Time response of microinverter by applying a power step change from 50% to 100% of rated power

## V. CUNCLUSION

Single phase single stage grid connected PV microinverters need big size PV side capacitor as energy buffering to compensate their output power pulsation. Electrolytic big size capacitors reduce the microinverter lifetime and reliability. In addition low frequency voltage ripple across this capacitor degrades PV utilization and raise output current THD. In this paper a new parallel active power decoupling circuit based on bidirectional flyback topology is proposed to reduce the aforementioned capacitor size and eliminate PV voltage ripple. Reducing capacitor sizes allows using film capacitors substitute of electrolitic capacitors. The proposed circuit operates as a controlled current source converter and ensures microinverter's required variable current. This circuit has very simple controller and does not need any additional feedbacks and sensors. Besides using proposed circuit enhances the PV utilization (by improving MPPT efficiency due to eliminating PV voltage ripple) and decreases capacitor power losses, therefore extra power loss at power decoupling circuit will be compensated. This decoupling circuit is employed with a single stage microinverter and its proper operation is verified by simulation using PowerSim software.

## REFERENCES

[1] A. C. Nanakos, G. C. Christidis and E. C. Tatakis, "Weighted Efficiency Optimization of Flyback Microinverter Under Improved Boundary Conduction Mode (i-BCM)," in *IEEE Transactions on Power Electronics*, vol. 30, no. 10, pp. 5548-5564, Oct. 2015.

[2] Y. H. Kim, J W. Jang, S. C. Shin and C. Y. Won, "Weighted-Efficiency Enhancement Control for a Photovoltaic AC Module Interleaved Flyback Inverter Using a Synchronous Rectifier," in IEEE Transactions on Power Electronics, vol. 29, no. 12, pp. 6481-6493, Dec. 2014.

[3] H. Hu, S. Harb, N. H. Kutkut, Z. J. Shen and I. Batarseh, "A Single-Stage Microinverter Without Using Eletrolytic Capacitors," in IEEE Transactions on Power Electronics, vol. 28, no. 6, pp. 2677-2687, June 2013.

[4] Y. H. Kim, S. C. Shin, J. H. Lee, Y. C. Jung and C. Y. Won, "Soft-Switching Current-Fed Push–Pull Converter for 250-W AC Module Applications," in *IEEE Transactions on Power Electronics*, vol. 29, no. 2, pp. 863-872, Feb. 2014.

[5] F. Edwin, W. Xiao and V. Khadkikar, "Topology review of single phase grid-connected module integrated converters for PV applications," *IECON 2012 - 38th Annual Conference on IEEE Industrial Electronics Society*, Montreal, QC, 2012, pp. 821-827.

[6] Z. Zhang, M. Chen, W. Chen, C. Jiang and Z. Qian, "Analysis and Implementation of Phase Synchronization Control Strategies for BCM Interleaved Flyback Microinverters," in *IEEE Transactions on Power Electronics*, vol. 29, no. 11, pp. 5921-5932, Nov. 2014.

[7] S. Zengin, F. Deveci and M. Boztepe, "Decoupling Capacitor Selection in DCM Flyback PV Microinverters Considering Harmonic Distortion," in *IEEE Transactions on Power Electronics*, vol. 28, no. 2, pp. 816-825, Feb. 2013.

[8] H. Hu, S. Harb, N. Kutkut, I. Batarseh and Z. J. Shen, "A Review of Power Decoupling Techniques for Microinverters With Three Different Decoupling Capacitor Locations in PV Systems," in *IEEE Transactions on Power Electronics*, vol. 28, no. 6, pp. 2711-2726, June 2013.

[9] F. Schimpf and L. Norum, "Effective use of film capacitors in single-phase PV-inverters by active power decoupling," *IECON 2010 - 36th Annual Conference on IEEE Industrial Electronics Society*, Glendale, AZ, 2010, pp. 2784-2789.

[10] S. B. Kjaer and F. Blaabjerg, "Design optimization of a single phase inverter for photovoltaic applications," *Power Electronics Specialist Conference, 2003. PESC '03. 2003 IEEE 34th Annual*, 2003, pp. 1183-1190 vol.3.

[11] H. Hu et al., "A Three-port Flyback for PV Microinverter Applications With Power Pulsation Decoupling Capability," in IEEE Transactions on Power Electronics, vol. 27, no. 9, pp. 3953-3964, Sept. 2012.

[12] G. C. Christidis, A. C. Kyritsis, N. P. Papanikolaou and E. C. Tatakis, "Investigation of Parallel Active Filters' Limitations for Power Decoupling on Single-Stage/Single-Phase Microinverters," in *IEEE Journal of Emerging and Selected Topics in Power Electronics*, vol. 4, no. 3, pp. 1096-1106, Sept. 2016.